OPEN ACCESS

Scholars International Journal of Chemistry and Material Sciences

Abbreviated Key Title: Sch Int J Chem Mater Sci
ISSN 2616-8669 (Print) | ISSN 2617-6556 (Online)
Scholars Middle East Publishers, Dubai, United Arab Emirates
Journal homepage: http://saudijournals.com

Original Research Article

Molecular Docking, Synthesis and Antimicrobial Evaluation of 4-[(3-hydroxybenzalidene)amino]antipyrine and its Copper Complex

Ilonwa Ifeanyichukwu[1], Ekpunobi Uche Eunice[1], Imomotimi Timipa Ajoko[2*], Tarinimi Tamunosa Jim-Halliday[3]

[1]Department of Pure and Industrial Chemistry, Nnamdi Azikiwe University, Awka, Anambra State, Nigeria
[2]Department of Chemical Sciences, Niger Delta University, Wilberforce Island, Bayelsa State, Nigeria
[3]Department of Chemistry, Faculty of Science, Rivers State University, Port Harcourt, Nigeria

DOI: 10.36348/sijcms.2023.v06i09.001 | **Received:** 19.10.2023 | **Accepted:** 23.11.2023 | **Published:** 29.11.2023

***Corresponding author:** Imomotimi Timipa Ajoko
Department of Chemical Sciences, Niger Delta University, Wilberforce Island, Bayelsa State, Nigeria

Abstract

The synthesis and characterization of Schiff base-containing transition metal complexes have gained increasing importance due to their catalytic roles in various reactions and their biological activities. These metal complexes have become crucial in drug design, leading to a growing interest in metal-based drugs. The study aimed to synthesize copper metal complex with a new Schiff base ligand 4-[(3-hydroxybenzalidene)amino]antipyrine derived from 4-aminoantipyrine and 3-hydroxybenzaldehyde, as well as evaluate their antimicrobial activity against gram positive and gram-negative bacterial strains. The ligand and its copper complex were assessed for antimicrobial activity against gram-positive and gram-negative strains utilizing disc diffusion and broth dilution methods. Spectroscopic techniques (UV-Vis, FT-IR, XRD, and EDXRF), solubility tests, and elemental analysis were employed to investigate the ligand and copper complex. The ligand displayed high insolubility in various solvents but had limited solubility in chloroform and methyl chloride. The FTIR spectrum of the Schiff base reveals the presence of aromatic hydrocarbons, imine (C=N), hydroxyl (-OH), secondary amine (C-N), carbonyl (C=O), and vibrations associated with C-O and C-C bonds, reflecting its molecular structure. In the EDXRF analysis, a prominent peak at 7.80 keV corresponding to copper was detected, indicating that copper is the most abundant element found in the ligand. XRD analysis demonstrated distinct crystal structures for both the ligand and its copper complex. The UV-Vis spectra of the ligand exhibited an absorption peak at a UV lambda max of 220 nm, indicating a $\pi \rightarrow \pi^*$ transition. In contrast, the absorption peaks observed in the copper complex indicated different transitions compared to the Schiff base. The MIC results indicated the copper complex's stronger antimicrobial activity than the Schiff base against tested bacteria. Molecular docking studies showed that the interaction energies of the synthesized compounds, particularly the ligand and copper complex, surpassed that of the well-known anti-diabetic drug, metformin.

Keywords: Antipyrine, Complex, Copper, 3-Hydroxybenzylideneamine, Schiff base, Synthesis, Transitions.

INTRODUCTION

Schiff bases are flexible ligands formed by condensing primary amines with carbonyl groups in diverse conditions and solvents; involve the elimination of water molecules [1]. Schiff bases hold a distinguished position within the field of medicinal chemistry [2]. In coordination chemistry, Schiff bases have been crucial as essential chelating ligands for various metal ions. The significance of Schiff bases as ligands has led to a growing interest in the synthesis and characterization of transition metal complexes in recent years [3]. Over the preceding two decades, coordination compounds, particularly those comprising metal complexes with Schiff bases as ligands, have been the focus of extensive and widespread research. Due to their importance to biological processes, up-normal magnetic characteristics, and development of novel structural features, Schiff base complexes have been extensively researched. The broad spectrum of metals, varied ligand types, and diverse geometries offered by metal-based compounds make them invaluable for exploring a largely uncharted chemical landscape in drug development. This is particularly significant in the context of designing innovative antimicrobial agents [4]. Metal complexes possess solubility in biological fluids due to the inherent tendency of metal atoms to relinquish electrons and acquire positive charges. As a result, drugs based on transition metals, in particular, present potential

advantages compared to the prevalent organic-based drugs [5- 7].

Schiff bases represent a captivating group of chelating ligands that has proven to be exceptionally beneficial in the coordination chemistry of both transition and inner transition metals. The Schiff bases derived from 4-aminoantipyrine and their complexes are recognized for their diverse applications in catalysis, clinical uses, and pharmacology [8]. Furthermore, antipyrine has discovered practical applications beyond the pharmaceutical domain, notably in tasks such as the solvent extraction of metal ions and as ligands within complexes exhibiting catalytic activity [9].

Schiff base complexes have garnered significant attention as a result of their chemical properties, structures, coordination behaviors, and diverse range of applications. With the versatile nature of Schiff bases and their complexes in mind, this study aimed to synthesize, characterize, and biologically evaluate transition metal complex using a Schiff base obtained from 4-aminoantipyrine and 4-hydroxybenzaldehyde.

EXPERIMENTAL METHOD

Synthesis of the Ligand (L)

4-aminoantipyrine (0.5mole, 9.16g) and 4-hydroxybenzaldehyde (0.5mole, 15.24g) were dissolved in 150 mL of ethanol. The mixture was stirred and refluxed at 85^{o}C for 2h and allowed to cool in ice. The mixture was subsequently filtered, rinsed with 200 mL of ethanol, and dried.

Synthesis of Cu (II) Complex of L

To a methanolic solution (100 mL) of 4-[(3-hydroxybenzalidene)amino]antipyrine (4 g) was mixed with a methanolic solution (100 mL) of $CuCl_2.2H_2O$ (2.50 g) with constant stirring for 30 min at room temperature. The mixture was refluxed for 2 hours and was subsequently cooled to room temperature. The resultant product was then obtained via filtration, rinsed with 200 mL of methanol, air-dried, and subsequently stored.

Solubility Test

The solubility assessment for the Schiff base was conducted in various solvents, including ethanol, methanol, chloroform, n-hexane, n-pentane, cyclohexane, methylene chloride, and distilled water. A small quantity of both Schiff base and copper (II) complex was added individually to the test tube, after which the solvent was introduced. Solubility was evaluated by agitating the test tube.

Infrared Spectral Analysis

The Fourier Transform Infrared (FTIR) spectra of the compound under investigation were recorded in the range of 4000-400cm^{-1} on Bulk Scientific model 530 FTIR Spectrometer. The compounds were prepared on KBr disc at spring board Research laboratory Awka.

UV-Visible Spectroscopy

The UV-visible spectra were measured within the 350-650 nm range at the Springboard Research Laboratory in Awka. The sample was dissolved in ethanol and then transferred into a cuvette before is been placed in the UV-spectrophotometer for absorbance detection.

EDX Scanning Electron Microscope SEM (PRO X)

This was done in Umaru Musa Yar'adua University Katsina state, Nigeria in the Central Research laboratory with Scanning Electron microscope model: PRO:X: 800-07334 Phenom World and serial number MVE01570775. It gives information regarding the structures, surface morphology of material.

X-ray Fluorescence Spectroscopy

The X-ray Fluorescence (XRF) analysis followed the standard procedure, utilizing Montana soil SRM 2710 as the reference material provided by Thermo Fisher Scientific. Each sample was weighed at 2 grams and then transferred into a sample holder, which was protected by a layer of cotton wool to avoid any spraying. The bottom of the sample holder is constructed from polypropylene, a thermoplastic material. The sample holders, each containing samples, underwent 10-minute vacuum process using a vacuum pump to eliminate oxygen and moisture. Subsequently, they were introduced into the XRF Spectrometer for chemical analysis. The method was calibrated using geological calibration of oxides in a vacuum in order to obtain the chemical analysis result in oxides. The samples were subjected to a 10-minute run in the XRF spectrometer, and the results were acquired thereafter.

Antimicrobial Susceptibility

The Disc Diffusion method was employed to assess the antimicrobial activities of both the ligand and the complex. Additionally, the minimum inhibitory concentrations (MIC) were established through the broth dilution method.

Standardization of Test Bacteria

The standardization of the test organisms involved using a sterile wire loop to select 3–5 pure cultures of the test microorganism, which were subsequently emulsified in 3–4 mL of sterile physiological saline. The absorbance of the 0.5 McFarland Standard was measured using a spectrophotometer at 540 nm. Concurrently, the turbidities of the test organisms were calibrated to correspond with the absorbance of the 0.5 McFarland standards at the same wavelength, utilizing physiological saline. NB: 0.5 McFarland contains 1.5 x 10^{8} cfu/ml.

Disc Diffusion Method

The evaluation of the extracts' antibacterial activities against the test bacteria was performed using modified disc diffusion methods [10- 13]. A precisely measured volume of 25 µL from a 0.5 McFarland standardized suspension of test bacteria ($1.5x10^8$ cfu ml^{-1}) was inoculated onto the Mueller-Hinton plates using the pour plate method. A precisely measured volume of 50 µL of the extracts was applied to saturate the 6mm filter paper discs, which were subsequently positioned on two distinct sections of the agar plate. The diameters of the inhibition zones on the different plates were evaluated and documented in millimeters. All experiments were carried out in triplicates. Negative controls were established using sterile physiological saline, while positive controls were established using 50 µg/ml Ciprofloxacin for bacteria and Nystatin for fungi.

Molecular Docking Studies

Docking Parameters

The docking study of the compounds was done over the crystal structure of diabetes mellitus proteins 2q5s and 3c45. The crystal structure of the main proteins was obtained from the protein data bank (PDB ID: 2q5s and 3c457: Resolution 1.49 Å and 2.05 Å, respectively) **[**14**]**. Possible docking modes between compounds and the protein were studied using the three virtual screening tools; PyRx- Python (2.6.5) Prescription 0.8, Biovia Discovery Studio v17.2.0.16349 and v20.1.0.19295. The grid used is at its maxima to cover the entire protein with Dimension (Å), X: 51.3737, Y: 66.9738 Z: 59.6069 and centre, X: -26.2840, Y: 12.5976, Z: 58.9679.

Selection of the Ligands and Preparation

The ligand and its copper complex together with one reference drug, metformin, were drawn on the ACD/Chem Sketch 17.1.2 [15]. The 2D structures of the two synthesised compounds including the reference drug (Fig 1) were imported onto the DS v17.2 and v20.1.

Molecular Docking

Auto-Dock Vina Incorporated into PyRx v2.6.4 was used to dock the selected compounds against the NtrC family transcriptional regulator (2Q5C and Human dipeptidyl peptidase IV/CD26 (3C45), in 8 exhaustiveness. Thereafter, the docked conformations with the highest binding affinity for each ligand and drug were imported onto the DS v17.2 and validated with v20.1. Discovery Studio (DS) v17.2 and v20.1, were recruited to evaluate the binding affinities existing between the protein and the ligands, and varied conformations were produced through the application of unpredictable rigid body rotation. In the end, the conformations with the least RMSD and highest binding energies were selected for analysis. Each binding affinity of the ligands including the drugs was analysed with parameters maintained at default. The-CDOCKER interaction energy was utilized to interpret the docking results [16], which signifies the energy associated with the non-bonded interactions between the protein and the ligand [17].

RESULTS AND DISCUSSION

Physical Characteristics

The ligand was yellow in color with a yield of 92% and a melting point of 56ºC. The significant yield suggests that the reaction is economically viable and shows promise. The Cu (II) complex was pale yellow in color with an appreciable percentage yield of 57% indicating the feasibility of the process of its synthesis. The ligand exhibited a notably high level of insolubility in various solvents, while showing limited solubility in chloroform and methyl chloride (Table 2). Some of the important physical properties of the ligand and the metal complex are shown in Table 1 and the solubility of the Ligand in Table 2.

Table 1: Physical properties of the ligand and its copper complex

Compound	Colour	% yield	Melting point
Ligand	Yellow	92%	56ºC
Copper complex	Pale yellow	57%	54ºC

Table 2: Solubility test of ligands and starting materials

Solvent	Ligand	4-aminoantipyrine	3-hydroxybenzaldehyde
Distilled water	Insoluble	Soluble	Soluble
Ethanol	Insoluble	Soluble	Soluble
Methanol	Insoluble	Soluble	Soluble
Chloroform	Sparingly soluble	Soluble	Soluble
Methylene chloride	Sparingly soluble	Soluble	Soluble
Cyclohexane	Insoluble	Soluble	Soluble
N-hexane	Insoluble	Soluble	Insoluble
N-pentane	Insoluble	Soluble	Soluble

Spectral Analysis

UV-Vis Studies of the Ligands and Their Metal Complexes

The UV-Vis spectra of the ligand and its Cu complex provide valuable information about their electronic transitions and structural properties. The UV lambda max of 220nm of the ligand suggests that the Schiff base exhibits a π→π* transition. This type of transition typically occurs due to the excitation of electrons from the non-bonding or weakly bonding π molecular orbitals to the corresponding π* anti-bonding orbitals.

Cu complex with absorption peaks at 221nm, 262.9nm, and 309.1nm: The absorption peaks observed in the Cu complex shows different electronic transitions compared to the Schiff base. The absorption at a slightly higher wavelength compared to the ligand suggests that the coordination of the Cu ion has influenced the electronic structure of the ligand. This shift in the absorption wavelength indicates the formation of a coordination bond between the Cu ion and the ligand. The absorption at this wavelength may correspond to a ligand-to-metal charge transfer (LMCT) transition. In this type of transition, an electron is promoted from the highest occupied molecular orbital (HOMO) of the ligand to the lowest unoccupied molecular orbital (LUMO) of the metal. The presence of this peak indicates that electron transfer occurs from the Schiff base to the Cu ion upon complex formation. This absorption peak could be associated with a metal-to-ligand charge transfer (MLCT) transition. In MLCT transitions, an electron undergoes excitation from an orbital associated with the metal to one associated with the ligand. This peak indicates the potential for electron transfer from the Cu ion to the Schiff base ligand.

Table 3: UV-visible electronic spectra data of the ligand and complex

Compound	ν_5	λ_5, nm	ν_4	λ_4, nm	ν_3	λ_3, nm	ν_2	λ_2, nm	ν_1	λ_1, nm	Absorption bands
Ligand	-	-			45454.5	220	-	-	30562.3	327.2	200-400
Cu-Ligand complex	-	-			45248.9	221	38037.3	262.9	32352.0	309.1	200-400

Infrared Spectra of the Ligand and Copper (II) Complex

The FTIR (Fourier Transform Infrared) spectrum of the Schiff base 4-[(3-Hydroxybenzylidene) amino]-1,5- dimethyl-2-phenyl-1H-pyrazol-3(2H)-one provides information about the functional groups and bonds present in the compound. The absorption in the 1446.2-1423.8 cm^{-1} range suggests the presence of a C-H bending vibration, which is commonly observed in aromatic compounds. It indicates the existence of aromatic hydrocarbon groups in the molecule. The absorption in 1617.7-1610 cm^{-1} range is associated with stretching vibration of the C=N bond. It confirms the presence of an imine (C=N) group in the Schiff base. This peak is a characteristic feature of the Schiff base structure. 3451.5 cm^{-1} absorption peak at this frequency indicates the presence of hydroxyl groups (-OH) or water (H_2O). It suggests the presence of an -OH functional group, which can be ascribed to the hydroxyl group connected to the aromatic ring. The absorption at 1543.1 cm^{-1} suggests the existence of a C-N bond, confirming the presence of a secondary amine group (-NH-) in the Schiff base. The absorption peak at 1736.9 cm-1 is associated with the stretching vibration of the carbonyl (C=O) group. It indicates the presence of a carbonyl functional group, likely originating from the pyrazolone ring in the Schiff base. The absorption at 1028.7 cm^{-1} indicates the existence of a C-O bond, suggesting the existence of a -OH group in the molecule. 1326.9-1215.1 cm^{-1} absorption range could be associated with aromatic C=C stretching vibrations.

The FTIR spectrum of the Schiff base indicates the presence of various functional groups and bonds, including aromatic hydrocarbons, C=N (imine), -OH, C-N (secondary amine), C=O (carbonyl), C-O, and C-C vibrations associated with the molecular structure. These results provide insights into the chemical composition and bonding within the Schiff base molecule, contributing to its characterization.

Table 4: Infra-Red data of the ligand and complex (cm^{-1})

Compound	ν, OH, H_2O cm^{-1}	ν,C-H sp^3 cm^{-1}	ν,C=O cm^{-1}	ν,C=N cm^{-1}	ν,C=C aromatic	ν,C-O cm^{-1}	ν,C-H aromatic
Ligand	3451.5	2932.85	1736.9	1610	1326.9	1028.7	1446.2
Cu-complex	3451.5	2931.90	1736.9	1610	1327.5	1028.7	1446.2

EDXRF Analysis of the Ligand and Copper Metal Complex

The Energy Dispersive X-ray Fluorescence (EDXRF) technique measures the characteristic X-ray emissions from elements present in a sample. In this case, the EDXRF analysis detected a peak corresponding to copper (Cu) at 7.80 keV with the highest percentage. Let's interpret and discuss this result:

Copper peak at 7.80 keV: The presence of a prominent peak at 7.80 keV indicates the detection of X-rays emitted by copper atoms in the sample. Each element emits characteristic X-rays at specific energies

when excited by an external source such as an X-ray beam. The energy value of 7.80 keV corresponds to the unique X-ray emission energy of copper. The high percentage of Cu suggests that it is the most abundant element detected by EDXRF in the analyzed sample. The percentage indicates the relative amount or concentration of copper compared to other elements present.

The presence of a strong and prominent copper peak with the highest percentage in the EDXRF analysis suggests that the sample contains a significant amount of copper. This result indicates the existence of copper either as a primary constituent or as a trace element within the sample.

However, it's important to note that EDXRF analysis only supplies details regarding the elemental makeup of the sample. It does not provide information regarding the molecular arrangement or chemical bonding of the elements. Therefore, further analysis techniques are typically required to determine the chemical form and complexation state of copper in the sample, such as X-ray diffraction (XRD) or X-ray absorption spectroscopy (XAS).

The EDXRF result (Fig 12) indicates the presence of a substantial amount of copper in the analyzed sample, as evidenced by the prominent copper peak at 7.80 keV with the highest percentage. Further analysis is necessary to explore the chemical and structural aspects of the copper species present.

XRD Analysis of the Ligand and Copper Metal Complex

The X-ray Diffraction (XRD) technique provides information about the crystal structure of a material by analyzing the diffraction pattern generated when X-rays interact with the sample. In this case, the XRD analysis of the ligand and its Cu complex resulted in different space groups: 200: pm-3 for the ligand and 14:p121/n1 for the Cu complex.

The space group 200: pm-3 indicates that the crystal structure of the ligand resembles that of sodium aluminum silicate. Sodium aluminum silicate is a compound consisting of sodium, aluminum, and silicon ions arranged in a specific pattern in a crystal lattice. This suggests that the ligand may have a similar arrangement of atoms, possibly forming a crystalline structure similar to sodium aluminum silicate.

The space group 14:p121/n1 indicates that the crystal structure of the Cu complex corresponds to Azurite. Azurite is a mineral with a deep blue color, and its crystal structure consists of copper, carbon, and oxygen ions arranged in a specific pattern in the crystal lattice. This suggests that the Cu complex has a crystal structure similar to Azurite, potentially arising from the coordination between the copper ion and the ligand.

These XRD results indicate that both the ligand and its Cu complex have distinct crystal structures. The ligand resembles more the crystal structure of sodium aluminum silicate, while the Cu complex resembles the crystal structure of Azurite. This difference in crystal structures suggests that the coordination of the copper ion in the complex may have influenced the arrangement of atoms and bonding within the ligand. This result suggests structural differences between the ligand and its Cu complex, indicating the influence of the coordination of the copper ion on the crystal structure.

Biological Studies

Antimicrobial Screening

The antimicrobial properties of the extracts were assessed against a panel of test microorganisms using modified disc diffusion methods. The microorganisms under investigation comprised two Gram-positive species, namely *Staphylococcus aureus* and *Enterococcus faecalis*, two Gram-negative species, *Escherichia coli and Enterobacter aerogenes*, as well as two fungi, *Candida albicans* and *Aspergillus niger*. Positive controls, represented by 50 µg/ml Ciprofloxacin for bacterial strains and Nystatin for fungal strains were included in the experimental setup. The research findings, as outlined in Table 5, showed distinct outcomes for the ligand and it's Cu-complex.

Table 5: Preliminary Antimicrobial Susceptibility Screening of Extracts

Test Bacteria	MEAN INHIBITION ZONE DIAMETERS (IZD) IN MILLIMETRES±STANDARD DEVIATION											
	Ligand			Cu			Positive control			Negative control		
	ϰ	y	Mean±SD	ϰ	y	Mean±SD	ϰ	y	Mean±SD	ϰ	y	Mean±SD
Staphylococcus aureus	7	9	8.00±1.41	25	21	23.00±2.83	31	34	32.50±2.12	0	0	0.00±0.00
Escherichia coli	0	0	0.00±0.00	8	11	9.50±2.12	27	28	27.50±0.71	0	0	0.00±0.00
Enterobacteraerogenes	0	0	0.00±0.00	18	20	19.00±1.41	33	30	31.50±2.12	0	0	0.00±0.00
Enterococcus faecalis	0	0	0.00±0.00	0	0	0.00±0.00	35	37	36.00±1.41	0	0	0.00±0.00
Aspergillus niger	15	17	16.00±1.41	16	19	17.50±2.12	21	23	22.00±1.41	0	0	0.00±0.00
Candida albicans	0	0	0.00±0.00	0	0	0.00±0.00	25	23	24.00±1.41	0	0	0.00±0.00

The ligand showed antibacterial activity against a single Gram-positive bacterium, *Staphylococcus aureus*, and antifungal activity against *Aspergillus niger*. This was confirmed through inhibition zone diameters

(IZDs) of 8.00±1.41 and 16.00±1.41, as shown in Table 5. Conversely, the Cu-complex proved a broader spectrum of antimicrobial activity, showing inhibitory effects against Staphylococcus aureus, *Escherichia coli, Enterobacter aerogenes, and Aspergillus niger,* but it did not exert any inhibition against *Enterococcus faecalis* (Gram-positive bacterium) or *Candida albicans* (fungus). The IZDs obtained were 23.00±2.83, 9.50±2.12, 19.00±1.41, and 17.50±2.1, respectively, for the microorganisms mentioned. Consequently, it was clear that the Cu-complex had higher inhibitory activity compared to its parent ligand. Notably, the positive control showed the most potent inhibitory effect, surpassing both the ligand and its Cu-complex (Table 5).

Table 6: Minimum Inhibitory Concentration (MIC) of the Extracts on the various test organisms

	Ligand ($mgml^{-1}$)				**Cu ($mgml^{-1}$)**				**Positive control ($mgml^{-1}$)**				**Negative control ($mgml^{-1}$)**			
Test Bacteria																
	500	250	125	62.5	500	250	125	62.5	500	250	125	62.5	500	250	125	62.5
Staphylococcus aureus	NT	NT	T	T	NT	NT	NT	T	NT	NT	NT	NT	T	T	T	T
Escherichia coli	-	-	-	-	NT	NT	T	T	NT	NT	NT	NT	T	T	T	T
Enterobacteraerogenes	-	-	-	-	NT	NT	T	T	NT	NT	NT	NT	T	T	T	T
Enterococcus faecalis	-	-	-	-	-	-	-	-	NT	NT	NT	NT	T	T	T	T
Aspergillus niger	NT	NT	T	T	NT	NT	T	T	NT	NT	NT	NT	T	T	T	T
Candida albicans	-	-	-	-	-	-	-	-	NT	NT	NT	NT	T	T	T	T

Key: T= turbidity**;** NT = No turbidity**;** - = Not performed

Table 6 presents the respective MICs for the ligand and its Cu-complex. In assessing the minimum inhibitory concentrations (MICs) of the compounds, similar trends to those observed with IZDs were clear, albeit with varying concentrations. The ligand showed the highest MICs (250 mg/ml) against the microorganisms it exhibited activity against, which corresponded to the IZDs recorded in the earlier analysis. Notably, the Cu-complex displayed identical MIC values to the ligand, except for its activity against *Staphylococcus aureus*, where the MIC value was 125 mg/mL. Coparatively, the positive control achieved the most notable inhibitory concentration of 62.5 mg/ml.

Furthermore, the modified disc diffusion methods revealed varying degrees of antimicrobial efficacy for the ligand and its Cu-complex against the tested microorganisms. The Cu-complex demonstrated a broader spectrum of inhibitory activity, while the ligand showed more limited antimicrobial effects, targeting a single Gram-positive bacterium and one fungus. Moreover, the positive control, represented by Ciprofloxacin and Nystatin, displayed the most pronounced antimicrobial potential in this investigation.

Molecular Docking Studies

Molecular Docking Mechanism

The compounds synthesized, along with the established anti-type 2 diabetes drug, Metformin, exhibited favorable results from the docking analysis conducted on the protein drug target. The docking analysis revealed that the interaction energies of these two compounds surpassed those of the known anti-diabetic candidate, Metformin, as illustrated in Table 7.

Table 7: Results of the docking of synthetic compounds on the crystal structure of 2Q5C receptor

Parameters	**Ligand**	**Cu-ligand complex**	**Metformin**
Binding Sites/Residue	ARG288, ASP197, LEU330, CYS285, ILE281, MET364, MET348, ILE341, VAL339289	PHE374, HIS435, LEU377, LYS230, LEU435, LEU421, LEU431, GLU378, ASP380, ASP383, LEU384,	ASP386, GLU324, GLN437, GLN410
Binding affinity (Kcal/mol)	-9.0	-9.4	-5.7
Number of bonded amino acid	8	8	4

Table 8: Results of the docking of synthetic compounds on the crystal structure of 3C45 receptor

Parameters	**Ligand**	**Cu-ligand complex**	**Metformin**
Binding Sites/Residue	ARG288, ASP197, LEU330, CYS285, ILE281, MET364, MET348, ILE341, VAL339289	PHE374, HIS435, LEU377, LYS230, LEU435, LEU421, LEU431, GLU378, ASP380, ASP383, LEU384,	ASN562, THR565, ARG560
Binding affinity (Kcal/mol)	-7.7	-8.9	-5.5
Number of bonded amino acid	5	7	3

The interaction energies (Kcal/mol), resulting from the docking of 2Q5C and 3C45 receptors were evaluated using PyRx docking simulations. The results were displayed in Table 7 for 2Q5C and Table 8 for 3C45. Notably, both the ligand and the Cu-complex demonstrated a higher inhibitory capacity in comparison to the reference drug metformin. The ligand showed interaction energies of -9.0 and -7.7 kcal/mol for 2Q5C and 3C45, respectively, while the Cu-complex exhibited energies of -9.4 and -8.9 kcal/mol for the same proteins. In contrast, metformin had lower interaction energies of -5.7 and -5.5 kcal/mol for 2Q5C and 3C45, respectively.

Considering the high binding energies observed for the Cu-complex, it is expected to possess greater inhibitory capacity than the ligand (-9.0 kcal/mol). This conclusion aligns with the findings of previous studies [18, 19], which suggest that ligand-protein interactions with higher binding affinity are indicative of increased inhibitory potential.

Metformin, a well-known FDA-approved anti-diabetic drug with proposed activity against Type-2 diabetes mellitus, served as the reference compound for screening the ligand and its metal complex. Moreover, a fascinating finding emerged during the study. Both the ligand and the control drug occupied a common binding pocket, but it was different from the pocket utilized by the Cu-complex. This discrepancy implies that the studied inhibitor and the reference drug might utilize different modes of inhibition [20].

The findings also highlight the superior inhibitory capacity of the Cu-complex compared to both the ligand and the reference drug metformin. This insight into their differential modes of action could pave the way for the development of more effective therapeutics for Type-2 diabetes mellitus.

The Binding Energies

Binding energies derived from the docking of 2Q5C and 3C45 were presented in Table 7 and 8. The ligand and its Cu-complex exhibited as the best potential inhibitors than metformin with higher binding energies than the known drug, metformin. A comparative performance study, with metformin as the reference molecule, serves as an indication substantiating the efficacy of the synthesized compounds. This shows that all the synthesized compounds have higher inhibitory property than the control drug, metformin.

Binding affinity which determines the efficacy of drug is a function of the stability of the protein-ligand complex formation and stability of protein-ligand complex. It is also dependent on the hydrophobic interaction and hydrogen-oxygen bonds (H-O) interactions stronger than those in water molecule [20]. By extension the greater the number of any of the non-covalent bond interactions the more stable the protein-ligand complex formed and the better the binding affinity. It is also observed that weaker H-O interactions (those with bond lengths greater than that in water molecule) cause reduction in protein-ligand complex stabilization, hence decrease in the binding energy of their interactions. The fact that the ligand and its Cu-complex have higher binding energies than the reference compound in their interactions with the 2Q5C and 3C45 receptors could be due to the nature and number of interaction they have with the amino residues present within the receptors' binding cavities. The synthesized compounds had 8 interactions with 5 kind of interactions (alkyl, pi-donor hydrogen bond, and pi-alkyl bonds) while the reference compounds established 4 bonds consisting of salt-bridge (Fig. 1-3), electrostatic, and hydrogen bond with the 2Q5C. In their interactions with the 3C45 receptor, the ligand and its Cu-complex 6 and 7 interactions, respectively with 4 kind on interactions (alkyl, pi-donor hydrogen bond, and pi-alkyl bonds) while the reference compounds established 6 bonds consisting mainly of conventional hydrogen bonds with the 3C45 (Fig.4-6).

The Binding Cavities and Interactions

Among the three docked compounds, only the Cu-complex exhibited a different binding pocket. This difference in binding pockets could be attributed to the larger size of the Cu-complex, which may have hindered its compatibility with the primary binding pocket of the receptors. Consequently, this suggests the possibility of the Cu-complex having a distinct mode of inhibition compared to the other compounds [21].

The reference drug, metformin, was found to interact with four (4) amino acids (Fig. 1) in the 2Q5C receptor, involving salt-bridge, electrostatic, and hydrogen bond interactions. In the case of the 3C45 receptor, metformin interacted with three (3) amino acids (Fig. 4), primarily forming hydrogen bonds.

In contrast, the ligand and its Cu-complex engaged with a greater number of amino acids within the binding cavity of receptor 2Q5C. Specifically, they formed interactions with eight (8) different amino acids, involving alkyl, pi-donor hydrogen bond, and pi-alkyl bonds (Fig. 2 and 3). For the 3C45 receptor, the ligand directly interacted with five (5) amino acids (Fig. 5), while its Cu-complex interacted with seven (7) amino acids within the receptor cavity (Fig. 6).

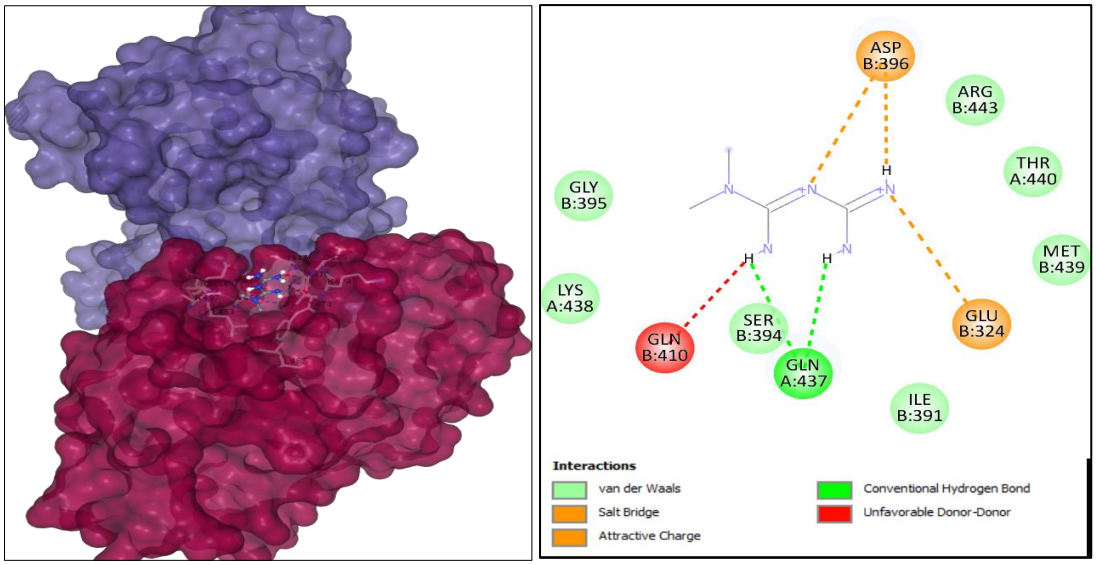

Fig. 1: Representation of docked ligand-protein complex 2D animation pose of REMD within the cavity of 2Q5C, and Interaction of Metformin with amino acid residues of Type-2 diabetes protein.

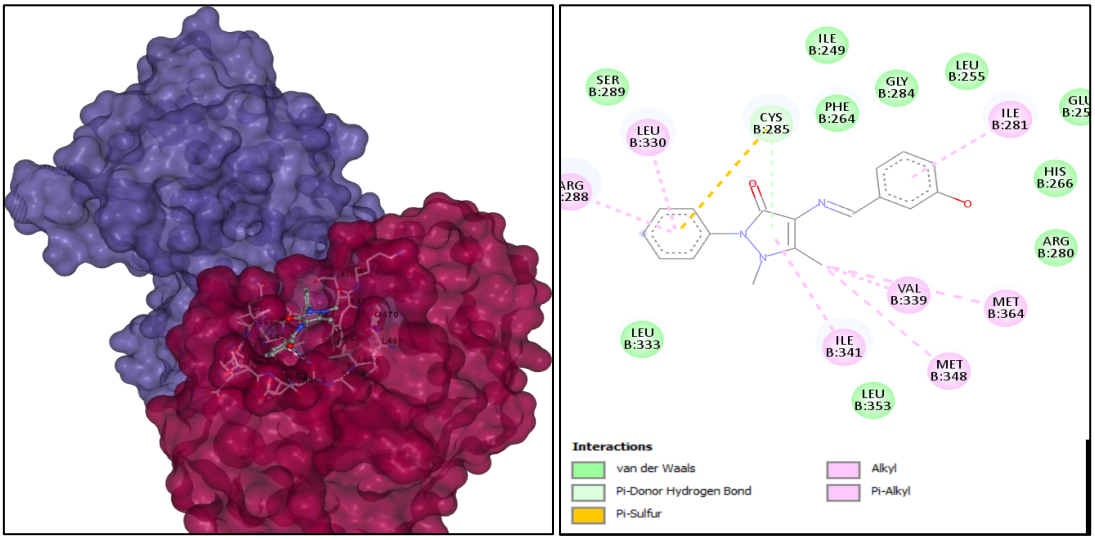

Fig. 2: Representation of docked ligand-protein complex 2D animation pose of REMD within the cavity of 2Q5C, and Interaction of Ligand with amino acid residues of Type-2 diabetes protein.

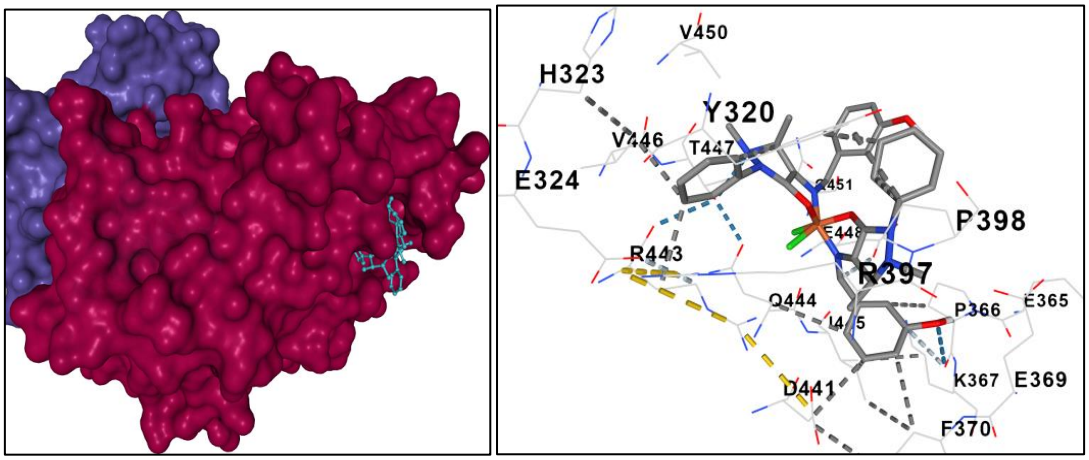

Fig. 3: Representation of docked ligand-protein complex 2D animation pose of REMD within the cavity of 2Q5C, and Interaction of Cu-complex with amino acid residues of Type-2 diabetes protein.

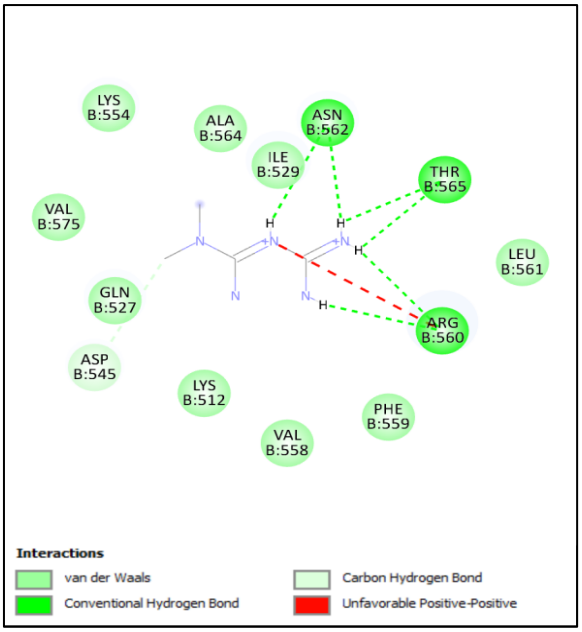

Fig. 4: Representation of docked ligand-protein complex 2D animation pose of REMD within the cavity of 3C45, and Interaction of Metformin with amino acid residues of Type-2 diabetes protein.

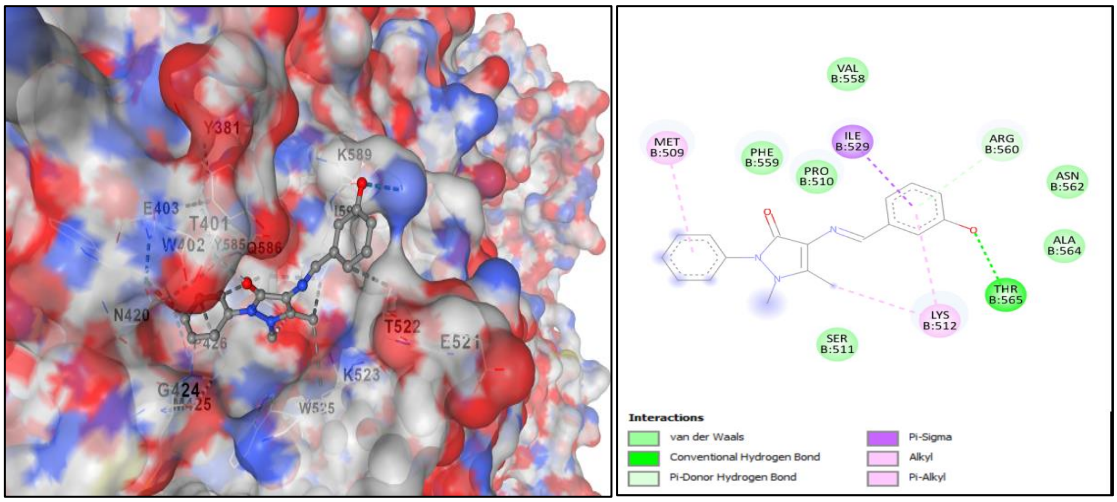

Fig. 5: Representation of docked ligand-protein complex 2D animation pose of REMD within the cavity of 3C45, and Interaction of Metformin with amino acid residues of Type-2 diabetes protein.

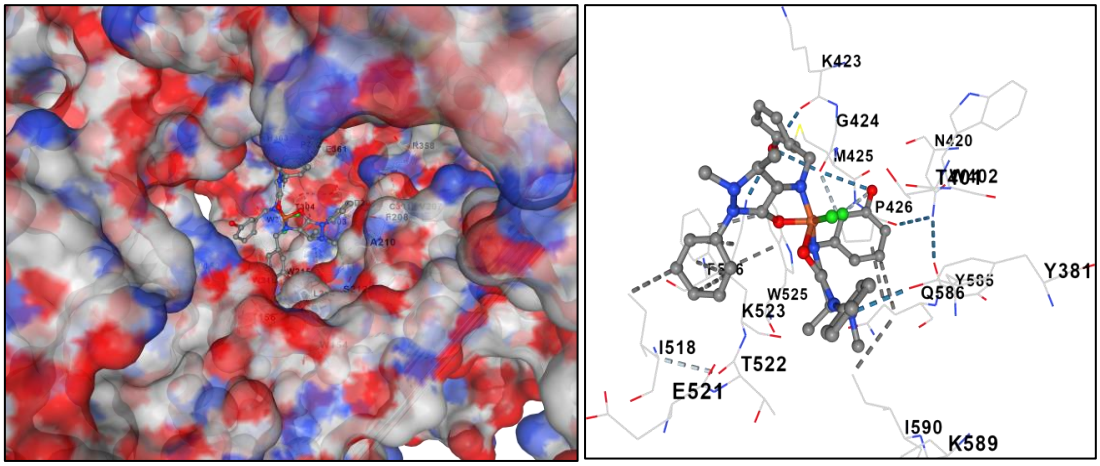

Fig. 6: Representation of docked ligand-protein complex 2D animation pose of REMD within the cavity of 3C45, and Interaction of Metformin with amino acid residues of Type-2 diabetes protein.

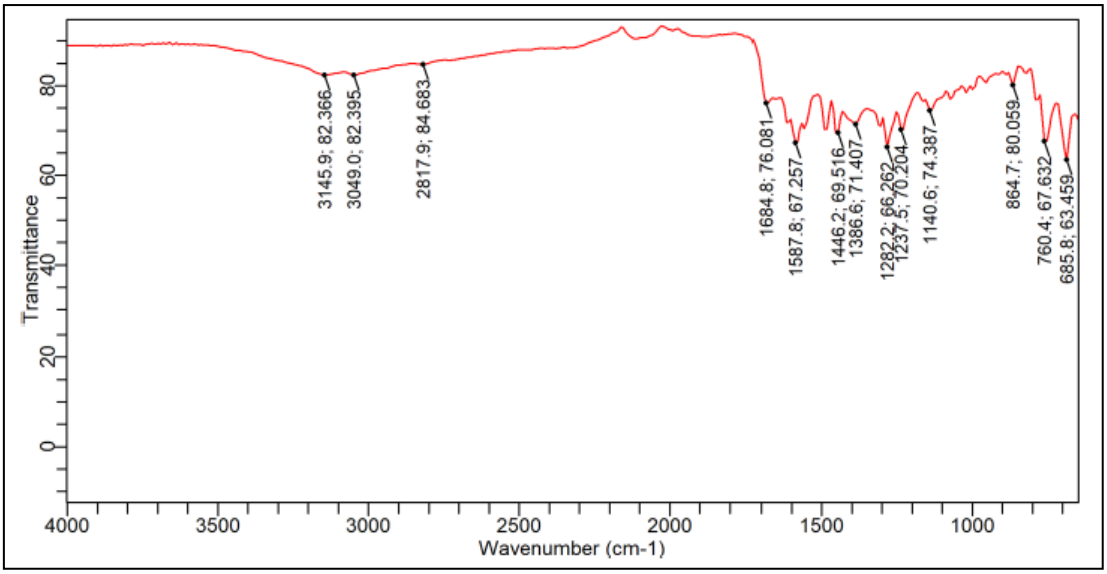

Fig 7: IR Spectrum of Copper Complex

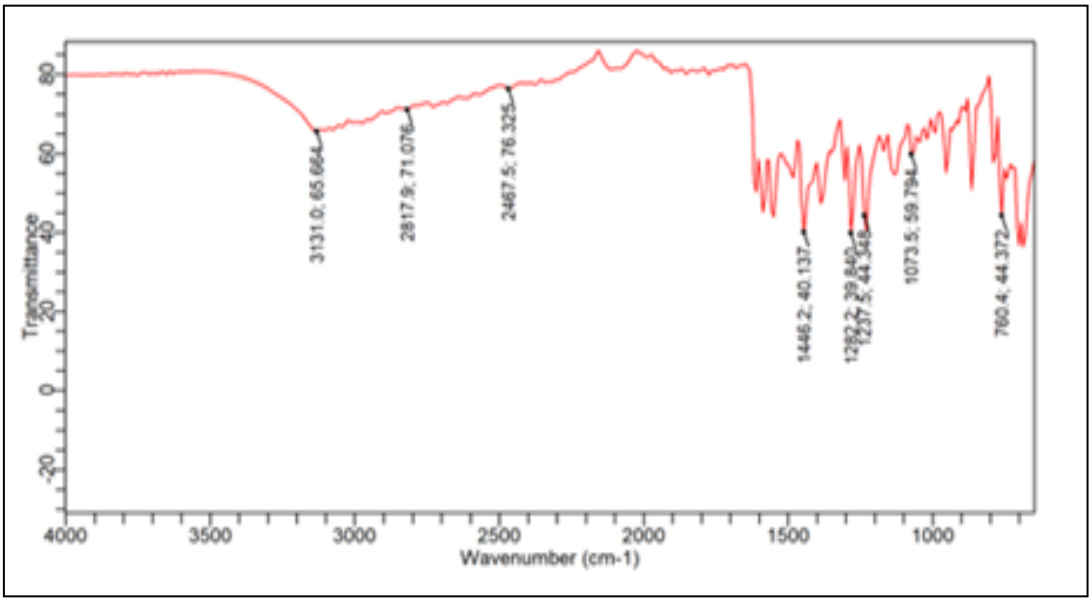

Figure 8: IR Spectrum of Ligand

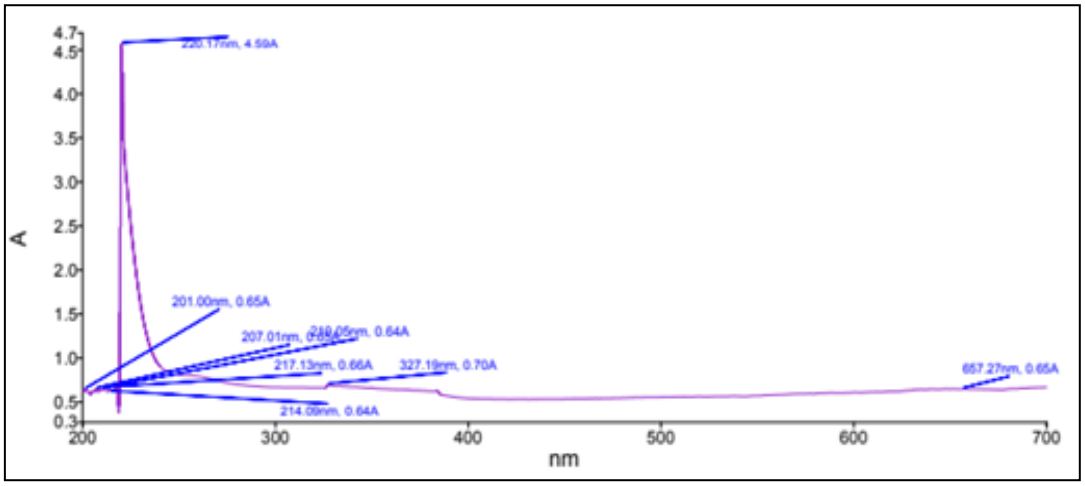

Figure 9: UV-vis spectra of Ligand

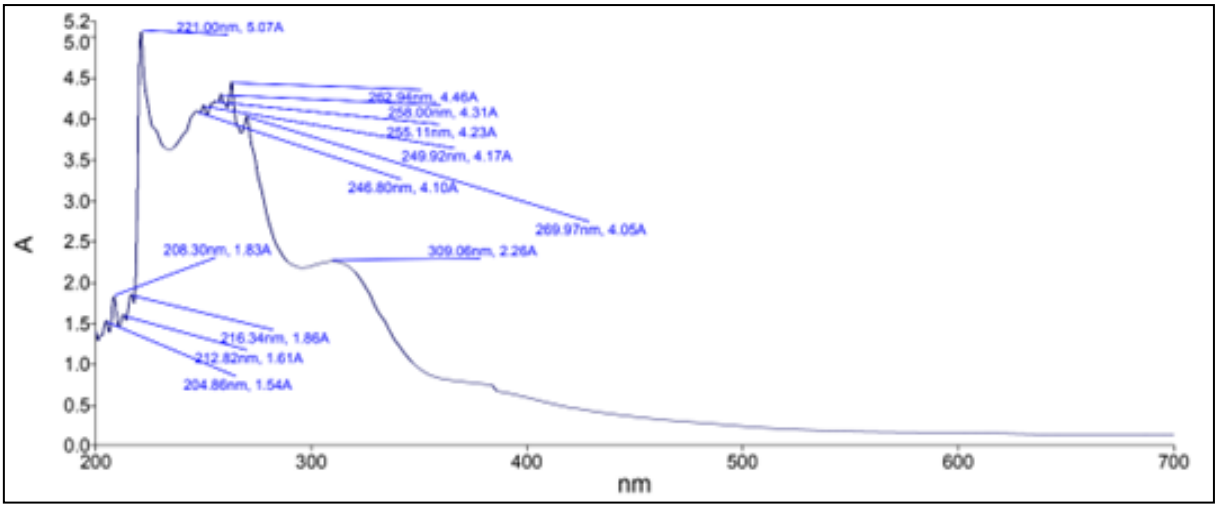

Figure 10: UV-vis spectra of Cu (II) complex

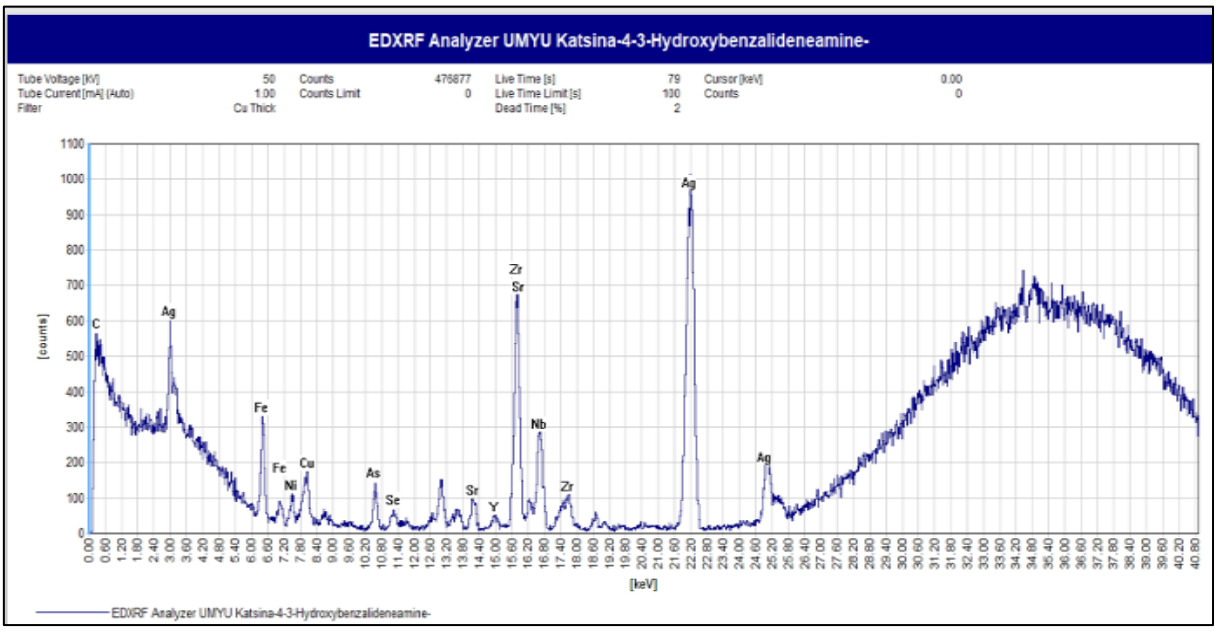

Figure 11: EDXRF Spectrum of Ligand

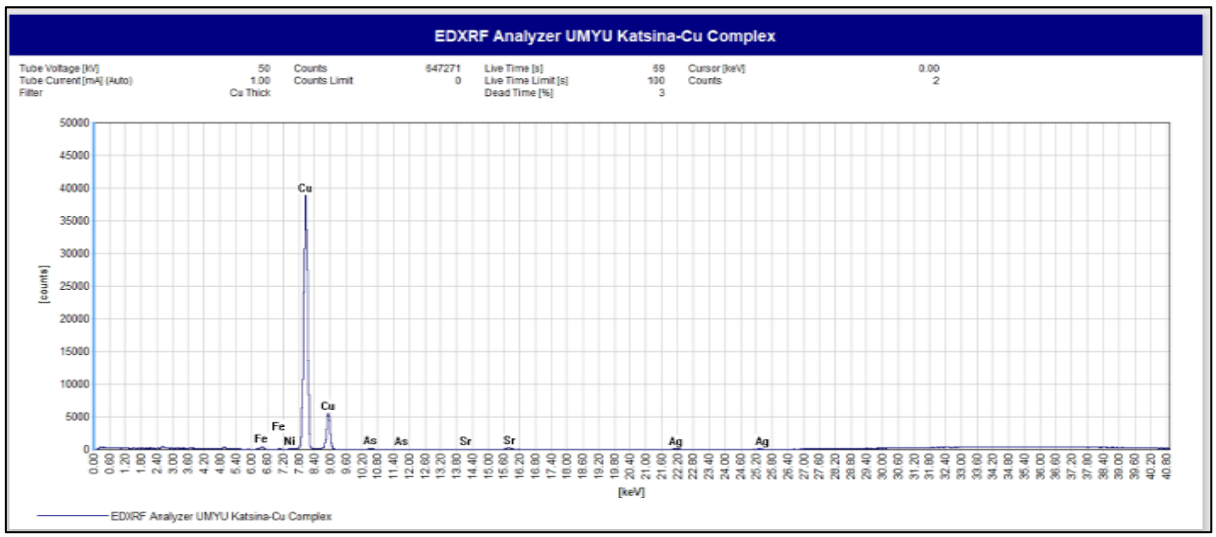

Figure 12: EDXRF Spectrum of Copper (II) Complex

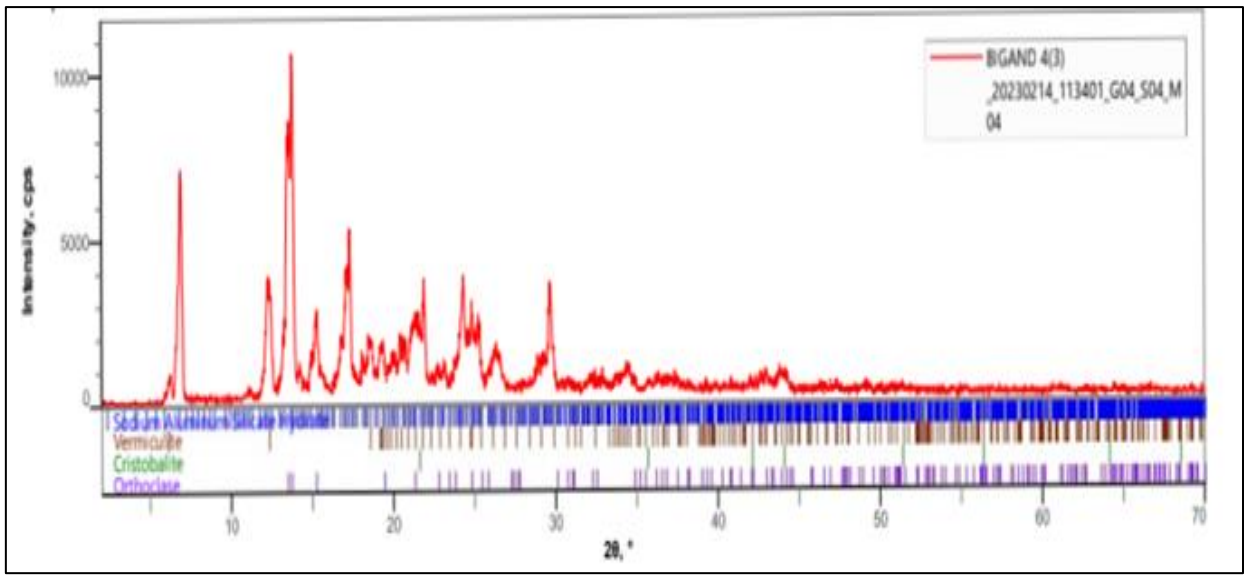

Figure 13: XRD Spectrum of Ligand

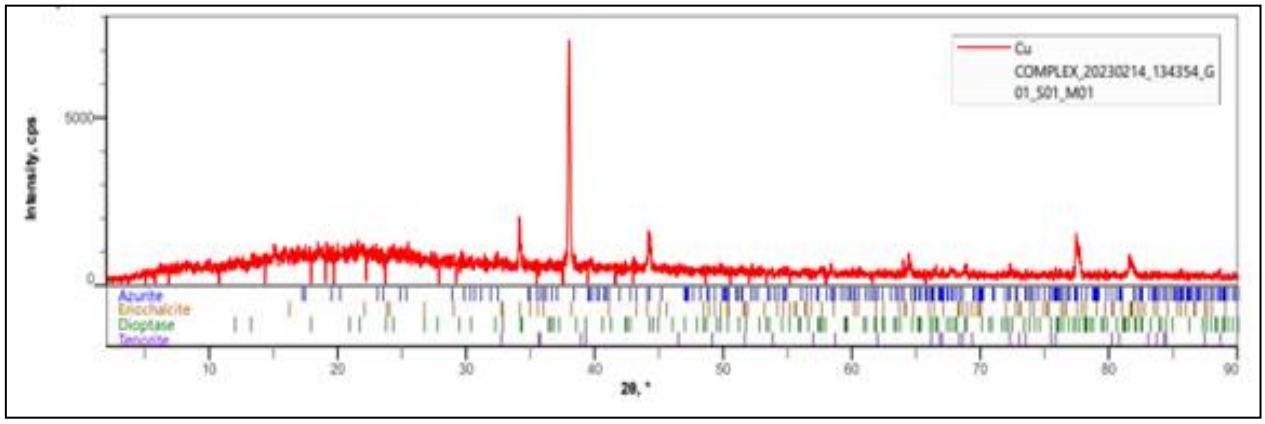

Figure 14: XRD Spectrum of Cupper (II) Complex

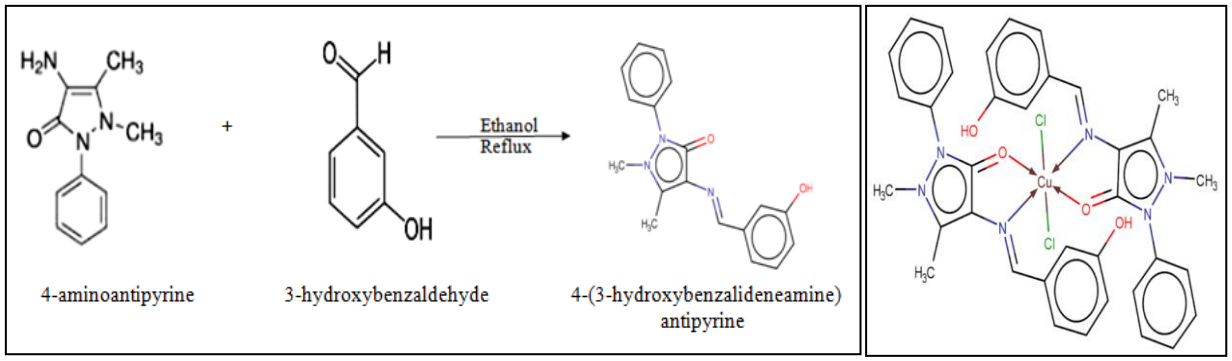

Figure 15: Proposed structure of the Copper complex

Scheme 1: Equation showing the synthesis of 4-[(3-hydroxybenzalidene)amino]antipyrine.

CONCLUSION

The study successfully synthesized and characterized 4-[(3-hydroxybenzalidene) amino] antipyrine and its copper complex, leading to valuable insights into their potential use as antimicrobial agents. The antimicrobial evaluation revealed that the copper complex exhibited higher antimicrobial activity compared to the ligand, 4-[(3-hydroxybenzalidene) amino] antipyrine. This observation indicates that the formation of the copper complex enhanced the antimicrobial properties of the ligand. Furthermore, the findings from molecular docking studies revealed that the synthesized compounds showed that the interaction energies of the ligand and copper complex were higher than the known anti-diabetic drug, metformin. This suggests that these

novel compounds possess greater potential as effective anti-diabetic agents than the existing drug metformin, making them promising candidates for future drug development efforts.

Conflicts of Interest: There are no conflicts of interest

REFERENCES

1. Nath, P., & Dhumwad, S. D. (2012). Antimicrobial studies of Co (II), Ni (II), Cu (II) and Zn (II) complexes derived from Schiff bases of 3-formyl quinoline and 3-hydrazinoquinoxalin-2 (1H) one. *Rasayan J Chem*, *5*(2), 234-8.
2. El-Barasi, N. M., Algazale, S. F., El-Ajaily, M. M., Maihub, A. A., Miloud, M. M., Al-Noor, T. H., ... & Kareem, M. M. (2023). Synthesis, characterization, theoretical study and biological evaluation of Schiff base and their La (III), Ce (IV) and UO2 (II) complexes. *Bulletin of the Chemical Society of Ethiopia*, *37*(2), 335-346.
3. Jishah, M. J., & Isac, S. R. C. (2017). Synthesis and characterization of Schiff base complexes of cu (II), Ni (II), Co (II) derived from furan 3-carboxaldehyde and 3-amino pyridine. *International Journal of scientific and research publication*, 7(10).
4. Morrison, C. N., Prosser, K. E., Stokes, R. W., Cordes, A., Metzler-Nolte, N., & Cohen, S. M. (2020). Expanding medicinal chemistry into 3D space: Metallofragments as 3D scaffolds for fragment-based drug discovery. *Chemical science*, *11*(5), 1216-1225.
5. Claudel, M., Schwarte, J. V., & Fromm, K. M. (2020). New antimicrobial strategies based on metal complexes. *Chemistry*, *2*(4), 849-899.
6. El-Tabl, A. S., Mohamed Abd El-Waheed, M., Wahba, M. A., & Abou El-Fadl, A. E. H. (2015). Synthesis, characterization, and anticancer activity of new metal complexes derived from 2-hydroxy-3-(hydroxyimino)-4-oxopentan-2-ylidene) benzohydrazide. *Bioinorganic chemistry and applications*, *2015*.
7. van Rijt, S. H., & Sadler, P. J. (2009). Current applications and future potential for bioinorganic chemistry in the development of anticancer drugs. *Drug discovery today*, *14*(23-24), 1089-1097.
8. Premnath, D., Selvakumar, P. M., Ravichandiran, P., Selvan, G. T., Indiraleka, M., & Vennila, J. J. (2016). Synthesis and spectroscopic characterization of fluorescent 4-aminoantipyrine analogues: Molecular docking and in vitro cytotoxicity studies. *Spectrochimica Acta Part A: Molecular and Biomolecular Spectroscopy*, *153*, 118-123.
9. Bao, R. D., Song, X. Q., Kong, Y. J., Li, F. F., Liao, W. H., Zhou, J., ... & Xie, M. J. (2020). A new Schiff base copper (II) complex induces cancer cell growth inhibition and apoptosis by multiple mechanisms. *Journal of Inorganic Biochemistry*, *208*, 111103.
10. Agu, K. C., Igweoha, C. A., & Umeh, C. N. (2013). Antimicrobial activity of the ethanolic and petroleum ether extracts of tangerine seed on selected bacteria. *International Journal of Agriculture and Biosciences*, *2*(1), 22-24.
11. Steve, A. C., Chidinma, O. L., Emmanuella, N. E., Chukwuebuka, A. K., Sunday, A. N., Chidi, O. B., & Nchedo, O. R. (2016). Phytochemical and antimicrobial screening of Cola gigantea leaves, stem and bark. *Univ. J. Microbiol. Res*, *4*, 49-54.
12. Awah, N. S., Agu, K. C., Okorie, C. C., Okeke, C. B., Iloanusi, C. A., Irondi, C. R., ... & Ekong, U. S. (2016). In-vitro assessment of the antibacterial quality of some commonly used herbal and non-herbal toothpastes on Streptococcus mutans. *Open Journal of Dentistry and Oral Medicine*, *4*(2), 21-25.
13. Awah, N. S., Agu, K. C., IIkedinma, J. C., Uzoechi, A. N., Eneite, H. C., Victor-Aduloju, A. T., ... & Ilikannu, S. O. (2017). Antibacterial activities of the aqueous and ethanolic extracts of the male and female Carica papaya leaves on some pathogenic bacteria. *Bioeng Biosci*, *5*(2), 25-29. DOI: 10.13189/bb.2017.050201.
14. Rampogu, S., & Rampogu Lemuel, M. (2016). Network based approach in the establishment of the relationship between type 2 diabetes mellitus and its complications at the molecular level coupled with molecular docking mechanism. *BioMed research international*, *2016*.
15. Ghosh, D., Griswold, J., Erman, M., & Pangborn, W. (2009). Structural basis for androgen specificity and oestrogen synthesis in human aromatase. *Nature*, *457*(7226), 219-223.
16. Fei, J., Zhou, L., Liu, T., & Tang, X. Y. (2013). Pharmacophore modeling, virtual screening, and molecular docking studies for discovery of novel Akt2 inhibitors. *International journal of medical sciences*, *10*(3), 265.
17. Fatima, A., Abdul, A. B. H., Abdullah, R., Karjiban, R. A., & Lee, V. S. (2015). Binding mode analysis of zerumbone to key signal proteins in the tumor necrosis factor pathway. *International Journal of Molecular Sciences*, *16*(2), 2747-2766.
18. Vijesh, A. M., Isloor, A. M., Telkar, S., Arulmoli, T., & Fun, H. K. (2013). Molecular docking studies of some new imidazole derivatives for antimicrobial properties. *Arabian Journal of Chemistry*, *6*(2), 197-204.
19. Wang, G., He, D., Li, X., Li, J., & Peng, Z. (2016). Design, synthesis and biological evaluation of novel coumarin thiazole derivatives as α-glucosidase inhibitors. *Bioorganic Chemistry*, *65*, 167-174.
20. Tomi, I. H., Al-Daraji, A. H., Abdula, A. M., & Al-Marjani, M. F. (2016). Synthesis, antimicrobial and docking study of three novel 2, 4, 5-triarylimidazole derivatives. *Journal of Saudi chemical society*, *20*, S509-S516.
21. Kellogg, G. E., Burnett, J. C., & Abraham, D. J. (2001). Very empirical treatment of solvation and

entropy: a force field derived from log Po/w. *Journal of Computer-Aided Molecular Design*, *15*, 381-393.